

## Extension of the TDCR model to compute counting efficiencies for radionuclides with complex decay schemes

K. Kossert<sup>a,\*</sup>, Ph. Cassette<sup>b</sup>, A. Grau Carles<sup>c</sup>, G. Jörg<sup>d,e</sup>, Christoph Lierse V. Gostomski<sup>e</sup>, O. Nähle<sup>a</sup>, Ch. Wolf<sup>f</sup>

<sup>a</sup> Physikalisch-Technische Bundesanstalt (PTB), Bundesallee 100, 38116 Braunschweig, Germany

<sup>b</sup> Laboratoire National Henri Becquerel, CEA-LNHB, CE-Saclay, 91191 Gif sur Yvette Cedex, France

<sup>c</sup> C/Voluntarios Catalanes, 62, 28039 Madrid, Spain

<sup>d</sup> Klinik und Poliklinik für Nuklearmedizin, Universitätsklinikum Würzburg, Oberdürrbacher Straße 6, 97080 Würzburg, Germany

<sup>e</sup> Radiochemie München (RCM), Technische Universität München, Walther-Meißner-Str. 3, 85748 Garching, Germany

<sup>f</sup> Naturwissenschaftlich-Technische Akademie (NTA), Seidenstr. 12-35, D-88316 Isny, Germany

### HIGHLIGHTS

- The TDCR model was extended to complex decay schemes.
- $\beta^-$  transitions with up to seven coincident  $\gamma$  transitions can be calculated.
- The extensions were tested using  $^{59}\text{Fe}$ ,  $^{64}\text{Cu}$ ,  $^{166\text{m}}\text{Ho}$  and  $^{229}\text{Th}$ .
- Further improvements of the models are required.

### ARTICLE INFO

Available online 13 November 2013

Keywords:

Activity standardization

Radionuclides with complex decay scheme

Free parameter model

TDCR

Ionization quenching

### ABSTRACT

The triple-to-double coincidence ratio (TDCR) method is frequently used to measure the activity of radionuclides decaying by pure  $\beta$  emission or electron capture (EC). Some radionuclides with more complex decays have also been studied, but accurate calculations of decay branches which are accompanied by many coincident  $\gamma$  transitions have not yet been investigated.

This paper describes recent extensions of the model to make efficiency computations for more complex decay schemes possible. In particular, the MICELLE2 program that applies a stochastic approach of the free parameter model was extended. With an improved code, efficiencies for  $\beta^-$ ,  $\beta^+$  and EC branches with up to seven coincident  $\gamma$  transitions can be calculated. Moreover, a new parametrization for the computation of electron stopping powers has been implemented to compute the ionization quenching function of 10 commercial scintillation cocktails.

In order to demonstrate the capabilities of the TDCR method, the following radionuclides are discussed:  $^{166\text{m}}\text{Ho}$  (complex  $\beta^-/\gamma$ ),  $^{59}\text{Fe}$  (complex  $\beta^-/\gamma$ ),  $^{64}\text{Cu}$  ( $\beta^-$ ,  $\beta^+$ , EC and EC/ $\gamma$ ) and  $^{229}\text{Th}$  in equilibrium with its progenies (decay chain with many  $\alpha$ ,  $\beta$  and complex  $\beta^-/\gamma$  transitions).

© 2013 Elsevier Ltd. All rights reserved.

### 1. Introduction

In liquid scintillation (LS) counting, the triple-to-double coincidence ratio (TDCR) method is a direct activity measurement method, in which the detection efficiency is calculated from a physical and statistical model of the photon distribution emitted by the scintillating source (Broda et al., 2007). The method was first developed for pure  $\beta$  emitting radionuclides (Pochwalski et al., 1988) and electron-capture (EC) nuclides with low atomic

number (Broda and Pochwalski, 1992). The TDCR method is based on the same assumptions which form the basis for the CIEMAT/NIST efficiency tracing technique (Grau Malonda, 1999). Despite the similarities of the two methods, most programs for the computation of the counting efficiencies were mainly developed for only one of these techniques. Several successful attempts were made to extend the CIEMAT/NIST method for activity standardizations of radionuclides with very complex decay schemes; in particular, analytical procedures for  $\beta$  transitions in coincidence with several  $\gamma$  transitions were developed (Günther, 1994; Oropesa Verdecia and Kossert, 2009), but comparable procedures are not yet available for the TDCR method. An interesting alternative to the analytical efficiency computation was developed by

\* Corresponding author. Tel.: +49 531 592 6110; fax: +49 5315 926 305.  
E-mail address: [Karsten.Kossert@ptb.de](mailto:Karsten.Kossert@ptb.de) (K. Kossert).

Grau Carles (2007), who presented the MICELLE code which applies a new stochastic approach. The main idea of this approach was to realize a sophisticated computation of the electron spectra created as a consequence of an EC process. The atomic rearrangement subsequent to an EC is very complex and, so far, analytical models have failed, in particular when the M atomic sub-shells or higher shells were included. The MICELLE code can also be used for pure  $\beta$  emitters and  $\beta$  transitions in coincidence with up to two  $\gamma$ /IC transitions (IC = internal conversion). In a recent work, Kossert and Grau Carles (2010) have extended the MICELLE program to also make calculations of triple and double counting efficiencies in a TDCR counter possible. In this way, the TDCR and the CIEMAT/NIST methods can be applied with the same model and the same nuclear input data.

In this work, further improvements of the TDCR model are presented. The MICELLE code was extended to take more coincident  $\gamma$ /IC transitions into account. The model was improved and a new method for the computation of ionization quenching has been included in the code.

In addition, the computation of energy spectra absorbed by the scintillator is discussed.

The applicability of the TDCR method for activity measurements of radionuclides with complex decay schemes is demonstrated by experimental studies.

## 2. Extensions of the TDCR model

The stochastic approach used in the MICELLE code performs an event-by-event simulation of all decay processes. In this way, the number of electrons per decay event and the respective electron energies are calculated and then used to compute the double counting efficiency of systems with two photomultiplier tubes (PMT), or the double and triple counting efficiencies of systems with three PMTs. The electrons may stem from  $\beta^-$  decay, IC or EC decay which may cause releasing of Auger electrons and Coster-Kronig electrons. Positrons from  $\beta^+$  transitions are treated in the same way as electrons. In addition, the interaction of  $\gamma$ -rays, annihilation photons or X-rays can cause an energy transfer to secondary electrons which also contribute to the counting efficiencies. Details about the stochastic approach and further developments have been previously published (Grau Carles, 2007; Kossert and Grau Carles, 2010).

### 2.1. 2.1 Extension to compute decay schemes with more coincident $\gamma$ /IC transitions

The previous MICELLE2 version makes computations of several decay types possible. The decay is defined by the parameter ICON in the control file CTL.DAT. It is possible to compute 1  $\beta$  transition with up to 2 coincident  $\gamma$ /IC transitions (parameter ICON=9), 1 EC with up to 3  $\gamma$ /IC transitions (ICON=11) and 1  $\beta^+$  with 1 coincident  $\gamma$ /IC transition. All in all, there were 14 possibilities for the ICON parameter. In this work, this has been extended according to Table 1 which comprises 10 new possibilities. The extension required considerable modifications to the program code. The computation of decay schemes with more  $\gamma$ /IC transitions requires the choice of the corresponding value for the parameter ICON as well as the required nuclear decay data for the  $\gamma$  transitions. As an example, Fig. 1 shows an input file for a  $\beta^-$ - $\gamma$ /IC- $\gamma$ /IC- $\gamma$ /IC- $\gamma$ /IC- $\gamma$ /IC calculation with ICON=18. The decay corresponds to one cascade (pathway from ground state of the mother isotope to ground state of the daughter isotope) in the decay of  $^{166\text{m}}\text{Ho}$ . The extensions of the program were realized in such a way that existing files with nuclear decay data still work. In this sense, the updated MICELLE version is backwards compatible.

**Table 1**

In MICELLE2 the computed decay scheme is defined by the parameter ICON. In this work, 10 new options were included in the extended MICELLE2 program.

Parameter ICON	Decay scheme
1	Pure EC
2	EC/ $\gamma$
3	EC- $\gamma$ /IC
4	Non-coincident EC- $\gamma$ /IC
5	$\gamma$ /IC
6	EC- $\gamma$ /IC- $\gamma$ /IC
7	$\gamma$ /IC- $\gamma$ /IC
8	$\beta^-$ - $\gamma$ /IC
9	$\beta^-$ - $\gamma$ /IC- $\gamma$ /IC
10	pure $\beta^-$
11	EC- $\gamma$ /IC- $\gamma$ /IC- $\gamma$ /IC
12	$\gamma$ /IC- $\gamma$ /IC- $\gamma$ /IC
13	Pure $\beta^+$ (2 annihilation photons are taken into account)
14	$\beta^+$ - $\gamma$ /IC (2 annihilation photons are taken into account)
15	$\beta^-$ - $\gamma$ /IC- $\gamma$ /IC- $\gamma$ /IC
16	$\beta^-$ - $\gamma$ /IC- $\gamma$ /IC- $\gamma$ /IC- $\gamma$ /IC
17	$\beta^-$ - $\gamma$ /IC- $\gamma$ /IC- $\gamma$ /IC- $\gamma$ /IC- $\gamma$ /IC
18	$\beta^-$ - $\gamma$ /IC- $\gamma$ /IC- $\gamma$ /IC- $\gamma$ /IC- $\gamma$ /IC- $\gamma$ /IC
19	$\beta^-$ - $\gamma$ /IC- $\gamma$ /IC- $\gamma$ /IC- $\gamma$ /IC- $\gamma$ /IC- $\gamma$ /IC- $\gamma$ /IC
20	$\beta^+$ - $\gamma$ /IC- $\gamma$ /IC (2 annihilation photons are taken into account)
21	EC- $\gamma$ /IC- $\gamma$ /IC- $\gamma$ /IC- $\gamma$ /IC
22	EC- $\gamma$ /IC- $\gamma$ /IC- $\gamma$ /IC- $\gamma$ /IC- $\gamma$ /IC
23	EC- $\gamma$ /IC- $\gamma$ /IC- $\gamma$ /IC- $\gamma$ /IC- $\gamma$ /IC- $\gamma$ /IC
24	EC- $\gamma$ /IC- $\gamma$ /IC- $\gamma$ /IC- $\gamma$ /IC- $\gamma$ /IC- $\gamma$ /IC- $\gamma$ /IC

A drawback of the stochastic approach is that the precision of the computed results depends on the number of simulated events. In the original MICELLE program the number of simulated events was limited to  $2 \times 10^4$ . The number of simulated decay events can be increased when the number of decay branches is low. However, the maximum number of events is few ( $10^5$ ) and depends on the computer architecture as well as the compiler and its options. For very complex decay schemes with many decay branches we propose a new procedure in which only one cascade is computed in one call of the MICELLE program. After computation, the files containing the results for the TDCR method and the CIEMAT/NIST method are stored and a new call of the MICELLE program is made to compute the next branch. Once all branches are calculated, the results are combined in an Excel sheet or with other tools. For  $^{166\text{m}}\text{Ho}$  the computation was realized by taking into account 30 cascades. Each of the cascades comprises one  $\beta$  transition and some comprise up to 6 coincident  $\gamma$ /IC transitions. The whole procedure is quite time consuming and the total computation time can be long (a few days, depending on the number of events, etc.), but the whole process can be partially automated with the aid of executable batch files.

As in the previous approach (Kossert and Grau Carles, 2010), the present model does not take into account any asymmetry effects, i.e. the PMTs are assumed to have the same quantum efficiency.

### 2.2. New parameterization of electron stopping powers and ionization quenching

Recently, Tan and Xia (2012) published new data on electron stopping powers in the range from 20 eV to 20 keV for the following 10 commercial scintillators: Optiphase HiSafe 2, Optiphase HiSafe 3, Insta-Gel Plus, Ultima Gold, Ultima Gold AB, Ultima Gold XR, Ultima Gold LLT, Ultima Gold MV, Ultima Gold F and Hionic-Fluor. The electron stopping power values are based on theoretical calculations applying a dielectric model including the Born-Ochkur exchange. Optical energy loss functions were empirically evaluated since experimental data are missing.

```

'Ho166m'      cascade 27/30

'
      BASIC DATA
'Decay scheme (1-15)      :      17
'Atomic data              :      'ER_ATOM.DAT'

''
      EC DECAY

'PK,PL1,PL2,PM           :      .0,.0,.0,.0
''
      BETA DECAY

'Endpoint energy          ='      73.5
'Mass number              ='      166.
'Daughter nucl. atomic number ='      68.
'Forbiddenness            ='      0
'Shape factor coefficients ='      0.,0.,0.
''
      GAMMA TRANSITIONS

'PGAM,EGAM (1)           :      0.9913,410.955
'PIK,PIL1,PIL2,PIL3,PIM (1) :      0.8462,0.1202,0.00,0.00,0.0336
'PGAM,EGAM (2)           :      0.9950,830.565
'PIK,PIL1,PIL2,PIL3,PIM (2) :      0.8270,0.1338,0.0,0.0,0.0392
'PGAM,EGAM (3)           :      0.9212,280.463
'PIK,PIL1,PIL2,PIL3,PIM (3) :      0.7170,0.2187,0.0,0.0,0.0643
'PGAM,EGAM (4)           :      0.7496,184.4107
'PIK,PIL1,PIL2,PIL3,PIM (4) :      0.6138,0.2946,0.00,0.00,0.0916
'PGAM,EGAM (5)           :      0.1266,80.580
'PIK,PIL1,PIL2,PIL3,PIM (5) :      0.2391,0.5812,0.00,0.00,0.1797
'PGAM,EGAM (6)           :      0.,0.

```

Fig. 1. File to define one cascade of the decay of  $^{166m}\text{Ho}$ . The cascade comprises one  $\beta$  transition and 6 coincident  $\gamma$ /IC transitions.

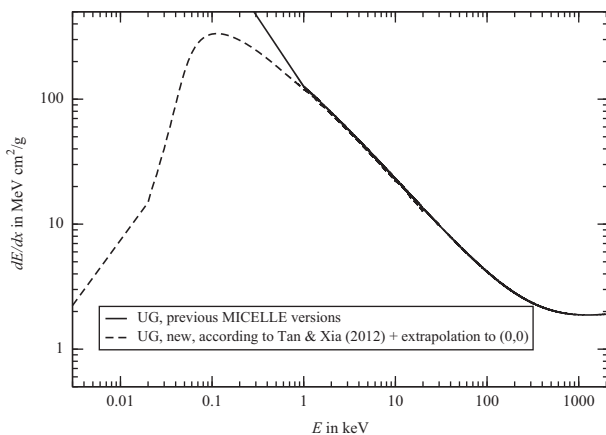


Fig. 2. Electron stopping power in Ultima Gold (UG) as a function of the kinetic electron energy. The curves were computed with the approach used in previous MICELLE2 versions (solid line) and with the new parameterization by Tan and Xia (2012) and extrapolation to (0, 0).

The stopping power values as tabulated by Tan and Xia were incorporated into the MICELLE2 program. A simple linear interpolation is used to compute stopping powers in the stated energy range between 20 eV and 20 keV. At the energy  $E=0$  keV, the stopping power is assumed to be  $0 \text{ MeV cm}^2 \text{ g}^{-1}$ , and between 0 eV and 20 eV a linear interpolation is used, too. The electron stopping powers were included for all 10 scintillators treated by Tan and Xia. In addition, the corresponding data of the 10 scintillators with atomic composition and density were added to the file SCINTL.DAT. These scintillators can be selected by using the scintillator option 7–16 in CTL.DAT. The composition data are also used for the simulation of the interactions of photons and should

not be changed to avoid inconsistencies. Fig. 2 shows the stopping powers for Ultima Gold compared to the previous approach which can still be selected in the program. This older approach has already been included in earlier versions of the MICELLE program (Grau Carles, 2007; Kossert and Grau Carles, 2010) and uses the electron stopping power calculation according to Rohrlich and Carlson (ICRU, 1984). For electron energies below 1 keV an empirical approach was used

$$\frac{dE}{dx} = \frac{dE}{dx|_{1 \text{ keV}}} E^{-1.1},$$

which leads to an increase in the electron stopping powers at low energies.

The stopping power calculation is used for numerical determination of the ionization quenching function. It is to be noted that the new parameterization only works with the scintillator compositions used by Tan and Xia (2012) since there would be inconsistencies otherwise. Fig. 3 compares the computed ionization quenching functions with the stopping power parameterization according to ICRU (1984) and the new approach. In both cases, the computations were made for Ultima Gold. When using the new approach, the electron stopping powers below 10 keV are calculated according to the dashed line in Fig. 2. Above 10 keV, the previous parameterization (solid line) according to ICRU (1984) is used which is very similar to the results from the ESTAR data base (ESTAR, 2013) when using the same atomic composition and density.

At the moment, it is not possible to judge which approach is better or more realistic. It is expected that the stopping power parameterization has a considerable influence on radionuclides which mainly emit electrons with low energies. A systematic investigation and a comparison have to be done in the near future.

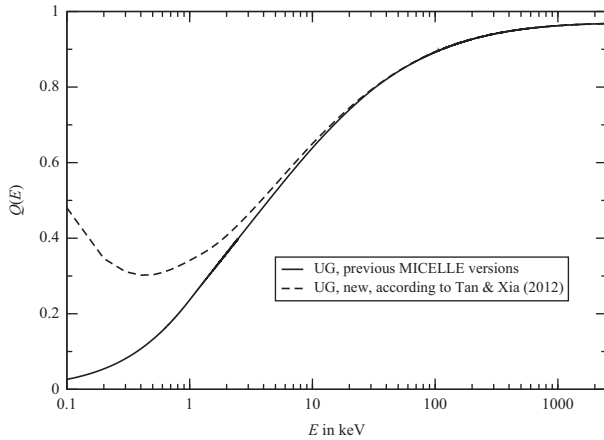


**Fig. 3.** The energy-dependent ionization quenching function in Ultima Gold (UG). The curves were calculated with different parameterizations of the electron stopping powers (Fig. 2).

### 2.3. Normalization of K-Auger and X-ray probabilities

The computation of atomic rearrangement as a consequence of EC or IC requires probabilities of all relevant Auger and X-ray transitions. The relative probabilities of K-shell Auger transitions are calculated using tabulated values from [Chen et al. \(1979\)](#). The X-ray emission probabilities are taken from [Browne and Firestone \(1986\)](#). These data are, however, not in full agreement with data evaluated by [Schönfeld and Janßen \(1996\)](#). In the current MICELLE program, a new subroutine reads atomic data as evaluated by [Schönfeld and Janßen \(1996\)](#); see [Table 1](#) in their original paper. In particular, the values  $u=2x$ ,  $v=x^2$  and  $x=P_K\beta/P_{K\alpha}$  are needed. The relative X-ray probabilities  $P_{KX}$  and  $P_{KL}$  as well as the relative Auger electron probabilities  $P_{KLL}$ ,  $P_{KLX}$  and  $P_{KXY}$  are then calculated applying

$$P_{KLL,ref} = (1+u+v)^{-1} P_{KLX,ref} = uP_{KLL} \quad P_{KXY,ref} = vP_{KLL}$$

$$P_{KL,ref} = 1/(1+x) \quad \text{and} \quad P_{KX,ref} = x/(1+x).$$

These values can be used to normalize the probabilities as defined in the file with atomic data. From this atomic data file we can compute the values (without normalization), e.g.

$$P_{KLL} = P'_{KL1L1} + P'_{KL1L2} + P'_{KL1L3} + P'_{KL2L2} + P'_{KL2L3} + P'_{KL3L3}.$$

The following normalization is then carried out:

$$P_{KL1L1} = P'_{KL1L1}/P_{KLL} \cdot P_{KLL,ref}$$

$$P_{KL1L2} = P'_{KL1L2}/P_{KLL} \cdot P_{KLL,ref}$$

$$P_{KL1L3} = P'_{KL1L3}/P_{KLL} \cdot P_{KLL,ref}$$

$$P_{KL2L2} = P'_{KL2L2}/P_{KLL} \cdot P_{KLL,ref}$$

$$P_{KL2L3} = P'_{KL2L3}/P_{KLL} \cdot P_{KLL,ref} \quad \text{and}$$

$$P_{KL3L3} = P'_{KL3L3}/P_{KLL} \cdot P_{KLL,ref}.$$

In the same manner, the values for KLX and KXY Auger electron probabilities are normalized ( $X > L$ ,  $Y > X$ ). For K-X-rays we use  $P_{KL} = P'_{KL2} + P'_{KL3}$  to apply the following normalization:

$$P_{KL2} = P'_{KL2}/P_{KL} \cdot P_{KL,ref} \quad \text{and}$$

$$P_{KX} = P'_{KM2} + P'_{KM3} + P'_{KM4} + P'_{KM5} \quad \text{to apply}$$

$$P_{KM2} = P'_{KM2}/P_{KX} \cdot P_{KX,ref}$$

$$P_{KM3} = P'_{KM3}/P_{KX} \cdot P_{KX,ref}$$

$$P_{KM4} = P'_{KM4}/P_{KX} \cdot P_{KX,ref} \quad \text{and}$$

$$P_{KM5} = P'_{KM5}/P_{KX} \cdot P_{KX,ref}.$$

The user of the program can define whether the normalization shall be carried out or not. A systematic investigation of the

influence of this normalization is still required. The influence depends on the radionuclide under study and the method. In the case of  $^{55}\text{Fe}$ , the normalization causes small changes when applying the CIEMAT/NIST method, but is negligible for the TDCR method. The new normalization is also interesting, since a comparison with the EMILIA code ([Grau Carles, 2006](#)) for low-Z EC nuclides is now more meaningful.

### 2.4. Calculation of the energy spectrum transferred to the scintillator

The effective energy spectrum to be considered when calculating the detection efficiency in the TDCR model is the spectrum of energy absorbed by the scintillator, which could differ from the energy spectrum of the radiations emitted by the radionuclide. These emissions comprise discrete X-rays,  $\gamma$ -rays, conversion and Auger electrons,  $\alpha$  particles or  $\beta^+$  and  $\beta^-$  particles. For particles with high stopping power and short range in the scintillator, it can be generally assumed that the whole particle energy is transferred to the scintillator. For high-energy electrons with kinetic energies of more than several hundreds of kiloelectronvolt, this assumption is not valid, since part of the particle energy can be lost in the vial walls, i.e. outside of the LS source. In this case, the energy released in the scintillator can be computed with the aid of Monte Carlo simulations. Nevertheless, it can be observed that when the path length of the electron is not negligible compared to the dimensions of the scintillating source, the energy of the particle is high and the associated detection efficiency in double or triple coincidences is close to unity, even if part of the energy is lost in the vial material. Thus, this case does not require a more sophisticated calculation of the spectrum absorbed by the scintillator.

The situation is very different for X-rays and  $\gamma$ -rays. Here, the spectrum of the energy absorbed by the scintillator must be calculated by means of Monte Carlo simulations. A detailed calculation is necessary, as the Compton interaction of photons with energies over a few tens of kiloelectronvolt is not negligible in an LS cocktail and, thus, a crude approximation using the total energy absorption and the interaction probability would not be accurate enough. This is why, in some recently developed TDCR calculation codes, a Compton interaction spectrum is calculated using the PENELOPE Monte Carlo code ([Salvat and Fernandez-Varea, 2009](#); [Salvat et al., 2011](#)). This code can be considered as a state-of-the-art simulation tool for the interaction of low-energy radiation in matter.

One important aspect in the simulation is the contribution of  $\gamma$  or X-rays scattered by the optical chamber structures, because some photons originally escaping from the source can be back-scattered by the walls of the counter and then re-enter the scintillator. For example, it has been shown that in the case of 835 keV  $\gamma$  radiation, these scattering effects induce a non-negligible increase of the absorption probability in the scintillator ([Cassette et al., 2006](#)).

The other effect to be taken into account is the calculation of the annihilation in flight for the positrons, when considering  $\beta^+$  decay. This could also be done using Monte Carlo simulation, but to reduce the simulation time, a specific module for the calculation of one quantum and two quanta annihilation in flight of the positron has been developed ([Lépy et al., 2010](#)). In the case of the  $^{64}\text{Cu}$   $\beta^+$  spectrum, with a maximum  $\beta$  energy of 653 keV, the annihilation in flight probability in the scintillator is about 0.6%.

Eventually, it will also be necessary to accurately calculate the shapes of  $\beta$  spectra. Up to now, it was considered that this is simple in the case of allowed spectra, but could be cumbersome for some forbidden transitions. The recent measurement of the  $^{63}\text{Ni}$  spectrum using magnetic microcalorimeters showed that two atomic effects, previously neglected, must also be taken into account: the exchange effect and the electron screening effect.



The exchange effect is the result of the creation of the  $\beta$  electron in an occupied atomic orbital of the daughter nucleus. This causes a distortion of the  $\beta$  spectrum at low energy. In the case of an unquenched  $^{63}\text{Ni}$  LS sample, this effect changes the calculated detection efficiency in a TDCR counter by about 0.8%.

The electron screening effect is related to the interaction of the  $\beta$  electron with the electrostatic field of the atomic electrons. Up to now, a simple correction model using a Thomas–Fermi potential was classically used, but this approach caused a non-physical discontinuity in the low-energy part of the spectrum. New models were developed to calculate this effect and it can be considered that for allowed transitions, more accurate  $\beta$  spectra models are now available. Nevertheless, the situation is not so comfortable for forbidden transitions and further developments are still needed in this field. The recent improvements also have not yet been included into the extended MICELLE2 code.

### 3. Applications of TDCR for activity determination of radionuclides with complex decay scheme

Experimental tests were performed to demonstrate that the TDCR method can be applied to radionuclides with complex decay schemes. Holmium-166m was selected to show that it is now possible to compute the counting efficiency of  $\beta$  transitions in coincidence with several  $\gamma$ /IC transitions. For the experimental test it was crucial to have an adequate  $^{166\text{m}}\text{Ho}$  solution without significant radioactive impurities available.

Additional measurements were carried out using  $^{59}\text{Fe}$ ,  $^{64}\text{Cu}$  and  $^{229}\text{Th}$ . With these isotopes it can be shown that the TDCR method can also be used for other decay types.

#### 3.1. $^{166\text{m}}\text{Ho}$

A  $^{166\text{m}}\text{Ho}$  solution was prepared at Radiochemie München of the Technische Universität München by means of thermal neutron activation of stable  $^{165}\text{Ho}$  and subsequent chemical purification. To this end, about 26 mg of high purity  $^{165}\text{Ho}_2\text{O}_3$  were irradiated for about 48 h at a thermal neutron flux  $\Phi$  of approximately  $1.1 \times 10^{14} \text{ s}^{-1} \text{ cm}^{-2}$ . The shorter-lived  $^{166}\text{Ho}$  ( $T_{1/2} = 26.795(29) \text{ h}$ ) is produced along with  $^{166\text{m}}\text{Ho}$ . From the ratio of the thermal neutron capture cross sections it can be expected that the corresponding number of produced  $^{166}\text{Ho}$  nuclei is very high. Thus, chemical purification procedures were started after 33 days. First  $\gamma$ -ray spectrometry measurements of the  $^{166\text{m}}\text{Ho}$  sample revealed the presence of  $^{160}\text{Tb}$  as the only photon-emitting impurity which had to be removed by means of ion chromatography using the complexing agent  $\alpha$ -hydroxyisobutyric acid. Due to only small variations in distribution coefficients among neighboring elements of the lanthanide series, long columns and small particle sizes are required to achieve satisfactory separation. After dissolution of  $\text{Ho}_2\text{O}_3$  in hot 8 M  $\text{HNO}_3$ , 100  $\mu\text{g}$   $\text{Tb(III)}$  were added and the solution was evaporated to dryness on a sand bath. The residue was taken up in 1 mL demineralized water and then applied to a 55 mL column filled with BioRad cation exchange resin AG 50W  $\times$  8, 10–40  $\mu\text{m}$  in  $\text{NH}_4^+$ -form.

Isocratic elution was subsequently performed by a solution of  $\alpha$ -hydroxyisobutyric acid of pH 4.7 and a flow of about 0.4 mL/min. The concentration of the eluent was 0.11 M until  $^{166\text{m}}\text{Ho}$  activity was detected in the effluent. The eluent concentration was then changed to 0.12 M until the complete elution of  $^{166\text{m}}\text{Ho}$ . The effluent was collected in fractions of 15 min each.

The  $^{166\text{m}}\text{Ho}$  fractions were checked for radiochemical purity by means of  $\gamma$ -ray spectrometry and the radiochemically pure fractions were combined and subsequently evaporated to dryness. In a subsequent chemical purification step, the  $\alpha$ -hydroxyisobutyric acid

was removed from the Ho-fractions in order to lower the salt content of the sample. The residue was taken up in 3 mL of 0.2 M HCl, the solution was then filtered through a pore size of 0.45  $\mu\text{m}$  and applied to a 3 mL column filled with Dowex 50W  $\times$  4, 50–100 mesh in  $\text{H}^+$ -form. The sample was run into the resin and the column was washed with 2 column volumes of 0.2 M HCl to rinse the  $\alpha$ -hydroxyisobutyric acid through the resin. The elution of Ho was effected by 16 column volumes of 10 M HCl Ultrapur<sup>®</sup>. The  $^{166\text{m}}\text{Ho}$  effluent was evaporated to dryness on a sand bath and the residue was analyzed by  $\gamma$ -ray spectrometry for radiochemical purity and estimation of the  $^{166\text{m}}\text{Ho}$  yield.

After these separation processes, further  $\gamma$ -ray spectrometry measurements of the sample confirmed that no photon-emitting radioactive impurity remained in the material, i.e. also  $^{160}\text{Tb}$  was removed completely.

An aliquot of the material was sent to PTB and measured by means of liquid scintillation counting in a custom-built TDCR counter and in two commercial counters for CIEMAT/NIST applications. For the computation of the counting efficiencies the decay scheme from Bé et al. (2004) was slightly simplified, taking into account 30 cascades. Seven  $\beta$  transitions and 22  $\gamma$ /IC transitions were included in the computation. The computed counting efficiencies of the individual cascades were combined in an Excel sheet using the normalized decay probabilities as weighting factor. The overall LS counting efficiency is rather high ( $> 98\%$ ) and, thus, low uncertainties can be expected. The high counting efficiency can be explained by the fact that each decay comprises one  $\beta$  electron and that most decays include the transition  $(\gamma/\text{IC})_{1,0}$  with a transition energy of about 80.6 keV (see, e.g., Bé et al., 2004). This latter transition mainly causes ejections of conversion electrons which are detected with high probability.

An LS sample was prepared with 1 mL of water and 15 mL of Ultima Gold. After a couple of days a slight cloudiness could be observed in the sample, in particular at the bottom of the vial. This sample instability is probably due to a relatively high salt concentration of the material. The determined activities of the TDCR and CIEMAT/NIST methods were in reasonable agreement with a relative deviation of about 0.2%. This deviation is mainly ascribed to the source instability. The deviation became slightly lower when the measurements were started directly after shaking the sample. The overall relative standard uncertainty of the activity was roughly estimated to be 0.3%. It can be concluded that the LS method can be used for activity standardization of this isotope. Thus, the described experiments were a good preparation for a new experiment to determine the half-life of  $^{166\text{m}}\text{Ho}$ , which is currently in progress as part of EMRP project “Radioactive Waste Management”.

#### 3.2. $^{59}\text{Fe}$

The extensions of the model were used to compute the counting efficiencies of  $^{59}\text{Fe}$ . The decay scheme of this isotope comprises 5  $\beta$  transitions and 7  $\gamma$  transitions, and there are 9 possible cascades. All transitions were taken into account for the efficiency computation. In 2012, an  $^{59}\text{Fe}$  solution was measured at PTB by means of the TDCR technique as well as using CIEMAT/NIST efficiency tracing. The results were in good agreement with a relative deviation of about 0.24 %. The CIEMAT/NIST efficiencies were calculated with the well-established analytical approach (Oropesa Verdecia and Kossert, 2009). If this approach is replaced with the stochastic model, the final result changes by less than 0.01%. This is an important confirmation of the stochastic approach.

An ampoule with about 3.6 g of the solution was sent to the BIPM to be measured in an ionization chamber of the International Reference System (SIR). The weighted mean of the two results was

used as final result with a relative standard uncertainty of only 0.16 %. Further details about the efficiency calculations, counters and sample preparation are described by Kossert and Nähle (in preparation).

### 3.3. $^{64}\text{Cu}$

The extensions were used to compute the detection efficiency of  $^{64}\text{Cu}$  which is a radionuclide of interest in nuclear medicine. It decays through three concurrent ways:  $\beta^+$ ,  $\beta^-$  and EC transitions. The TDCR method was applied by considering the weighted sum of calculated triple and double coincidence detection efficiencies for each branch. Two different nuclear and atomic data sets were used for the calculation of the detection efficiency, both derived from the “Table de radionucléides” but from different evaluations in 2004 (Bé et al., 2004) and more recently in 2010 (Bé et al., 2011). The differences between these evaluations mainly concern the probabilities of the  $\beta^-$ ,  $\beta^+$  and EC branches and, to a lesser extent, the energies of the transitions. As the relationship between the TDCR parameter and the detection efficiency is not a bijective function (one TDCR value can correspond to three values of detection efficiency), the identification of the relevant location on the efficiency vs. TDCR curve was obtained by making use of quenched sources and assuming that the effect of quenching is a decrease of the detection efficiency. The detection efficiency was then calculated, taking into account only the results of unquenched sources. The TDCR method was found to be very sensitive to the ratio of the EC probability over the sum of the  $\beta^+$  and  $\beta^-$  probabilities and it appeared that the determination of the detection efficiency was possible only with the ratio value derived from the new decay scheme from the 2010 evaluation (Bé et al., 2011). The relative standard uncertainty on the activity deduced from the TDCR measurement at LNH was 0.8 % (Table 2). An ampoule was sent to BIPM to be measured in an ionization chamber of the SIR. Further details on these measurements and results of the SIR are described by Bé et al. (2012) and Amiot et al. (2012).

### 3.4. $^{229}\text{Th}$

The TDCR method can also be applied to measurements of  $^{229}\text{Th}$  in radioactive equilibrium with its progenies. The decay chain comprises of several  $\alpha$  emitters as well as some complex  $\beta/\gamma$  radionuclides. The decay of the short-lived  $^{213}\text{Po}$  requires great care, since it often occurs during the dead time of the counter systems. The counting efficiency for single counts of  $^{213}\text{Bi}$  is

required to take this effect into account. Thus, the MICELLE program was modified to also compute the counting efficiency for the logical sum of single counts. Also the rather short-lived  $^{217}\text{At}$  may decay during the dead time caused by  $^{221}\text{Fr}$  decay events.

The overall counting efficiency of the TDCR system of PTB was found to be about 697%, depending on the degree of chemical quenching. The determined activity concentration was compared with the outcome of  $\alpha$  spectrometry under the defined solid angle (DSA) and the deviation between the two methods was found to be 0.38%. The relative standard uncertainties of the activity concentration were found to be about 0.23% and 0.7% for TDCR and DSA counting, respectively. Thus, both methods are in excellent agreement. Details about the efficiency computation and measurements with several counters are presented elsewhere (Kossert et al., accepted for publication).

## 4. Conclusion and outlook

It was demonstrated that the TDCR method can now be applied to activity measurements of radionuclides with complex decay schemes. This includes  $\beta$  emitting radionuclides, even when the  $\beta$  branches are in coincidence with up to seven  $\gamma/\text{IC}$  transitions. In addition, it was shown that radionuclides with complex decay chains comprising several  $\alpha$ ,  $\beta$  and  $\beta/\gamma$  transitions can be measured. However, the authors emphasize that the TDCR method is not necessarily the best choice for all isotopes. The results are often affected by some model dependence and accurate nuclear and atomic data are required to achieve reliable results, as shown in the case of  $^{64}\text{Cu}$ . Furthermore, the sample preparation can be complicated. In this sense, the liquid scintillation counting techniques should not be regarded as a substitute for other methods such as  $4\pi\beta\text{-}\gamma$  coincidence counting.

The current MICELLE version can also be used for the efficiency computation of low-Z EC nuclides. However, the extension towards higher atomic numbers still requires improvements in the atomic rearrangement simulation. The latest model contains some simplifications and the treatment of M, N and higher atomic shells needs to be improved. Moreover, the number of ejected electrons and their energies may be modulated by second-order effects like electron shake-up and shake-off. Photoionization, IC and EC usually remove an inner shell electron from the atom, leaving behind a perturbed ion in which the outer shell electrons may find themselves in a state that is not an eigenstate of the remaining atom. The resulting collective excitation is referred to as

**Table 2**  
Uncertainty budget for the activity determination of a  $^{64}\text{Cu}$  solution by means of TDCR.

Relative standard uncertainty contributions due to	$u_i \times 10^2$	
	Evaluation method A	Evaluation method B
Weighing and source dispersion	0.3	0.05
Dead time		0.01
Counting statistics	0.04	
Background	0.01	
Counting time		0.01
Impurities		Neglected (no impurity found)
Decay data and model		0.5
Adsorption		Neglected (no evidence of adsorption)
Ionization quenching parameter $k_B$		0.5
Sample (in)-stability		Neglected (no evidence of instability)
Half-life		0.04
Relative combined standard uncertainty, $u_c$	0.77	
Radioactivity concentration of the $^{64}\text{Cu}$ solution on the reference date of 18/3/2010, 12h00 UTC in kBq/g	Combined standard uncertainty in kBq/g	
817.4	6.3	

the electron shake-up effect. The excitation may cause emissions of low energy electrons from outer shells. This effect is called electron shake-off. Both effects have not yet been taken into account in the model.

There is also a need to improve the calculation procedures of  $\beta$  emission spectra. As for EC radionuclides, second-order effects like the exchange effect (Harston and Pyper, 1992) are to be considered. In particular, the counting efficiency of low-energy  $\beta$  emitters like  $^{241}\text{Pu}$  or  $^{63}\text{Ni}$  strongly depends on accurate spectra. At present, new procedures are being developed (Mougeot et al., 2011; Gorozhankin et al., 2011) and a new library of  $\beta$  spectra will be made available on the LNHBB web site.

## Acknowledgments

The extension of the TDCR model at PTB and CEA has been carried out within the scope of the EMRP Joint Research Project ENG08 “MetroFission”.

## References

- Amiot, M.N., Bé, M.-M., Branger, T., Cassette, Ph., Lépy, M.C., Ménesguen, Y., Da Silva, I., 2012. Nucl. Instrum. Methods Phys. Res. A 684, 97–104.
- Bé, M.-M., Chisté, V., Dulieu, C., Mougeot, X., Browne, E., Chechev, V., Kuzmenko, N., Kondev, F., Nichols, A., Luca, A., Galan, M., Arinc, A., Huang, X., 2011.  $^{64}\text{Cu}$  in Table of Radionuclides, Monographie BIPM-5, ISBN: 13 978 92 822 2234 8 (set) and ISBN: 13 978 92 822 2235 5 (CD), CEA/LNE-LNHBB, 91191 Gif-sur-Yvette, France and BIPM, Pavillon de Breteuil, 92312 Sèvres, France.
- Bé, M.-M., Chisté, V., Dulieu, C., Browne, E., Chechev, V., Kuzmenko, N., Helmer, R., Nichols, A., Schönfeld, E., Dersch, R., 2004. Table of Radionuclides, Monographie BIPM-5, ISBN: 92-822-2207-7 (set) and ISBN: 92-822-2205-5 (CD), CEA/BNM-LNHBB, 91191 Gif-sur-Yvette, France and BIPM, Pavillon de Breteuil, 92310 Sèvres, France.
- Bé, M.-M., Cassette, Ph., Lépy, M.C., Amiot, M.-N., Kossert, K., Nähle, O.J., Ott, O., Wanke, C., Dryak, P., Ratel, G., Sahagia, M., Luca, A., Antohe, A., Johansson, L., Keightley, J., Pearce, A., 2012. Standardization, decay data measurements and evaluation of  $^{64}\text{Cu}$ . Appl. Radiat. Isot. 70, 1894–1899.
- Broda, R., Pochwalski, K., 1992. The enhanced triple to double coincidence ratio (ETDCR) method for standardization of radionuclides by liquid scintillation counting. Nucl. Instrum. Methods Phys. Res. A 312, 85–89.
- Broda, R., Cassette, P., Kossert, K., 2007. Radionuclide metrology using LS counting. Metrologia 44, S36–S52.
- Browne, E., Firestone, R.B., 1986. Table of Radioactive Isotopes. Wiley, New York, p. 1986.
- Cassette, P., Ahn, G.H., Alzitzoglou, T., Aubineau-Lanière, I., Bochud, F., Garcia Torano, E., Grau Carles, A., Grau Malonda, A., Kossert, K., Lee, K.B., Laedermann, J.P., Simpson, B.R.S., van Wyngaardt, W.M., Zimmerman, B.E., 2006. Comparison of calculated spectra for the interaction of photons in a liquid scintillator. Example of  $^{54}\text{Mn}$  835 keV emission. Appl. Radiat. Isot. 64, 1471–1480.
- Chen, M.H., Crasemann, B., Mark, H., 1979. Relativistic radiationless transition probabilities for atomic K- and L-shells. At. Data Nucl. Data Tables 24, 13.
- ESTAR, 2013. (<http://physics.nist.gov/PhysRefData/Star/Text/ESTAR.html>).
- Gorozhankin, V., Bé, M.-M., Mougeot, X., Perevoshchikov, L.Briancon, Ch., 2011. Construction of beta spectrum on the basis of experimental nuclear decay data. In: Proceedings of the 2010 International Conference on Liquid Scintillation Spectrometry, Paris, France, Radiocarbon, The University of Arizona, Tucson, Arizona, USA, ISBN: 978-0-9638314-7-7, pp. 259–266.
- Grau Carles, A., 2006. EMILIA, the LS counting efficiency for electron-capture and capture-gamma emitters. Comput. Phys. Commun. 174, 35–46.
- Grau Carles, A., 2007. MICELLE, the micelle size effect on the LS counting efficiency. Comput. Phys. Commun. 176, 305–317.
- Grau Malonda, A., 1999. Free parameter models in LS counting. Colección Documentos CIEMAT. CIEMAT (1999), ISBN: 84-7834-350-4.
- Günther, E.W., 1994. Standardization of  $^{59}\text{Fe}$  and  $^{131}\text{I}$  by liquid scintillation counting. Nucl. Instrum. Methods Phys. Res. A 339, 402–407.
- Harston, M.R., Pyper, N.C., 1992. Exchange effects in  $\beta$  decays of many-electron atoms. Phys. Rev. A 45, 6282–6295.
- ICRU, 1984. Stopping powers for electrons and positrons. ICRU Report. International Commission on Radiation Units and Measurements, Bethesda, MD, USA, vol. 37, p. 5.
- Kossert, K., Grau Carles, A., 2010. Improved method for the calculation of the counting efficiency of electron-capture nuclides in LS samples. Appl. Radiat. Isot. 68, 1482–1488.
- Kossert, K., Nähle, O., 2013. Activity determination of  $^{59}\text{Fe}$ . In: Proceedings of the LSC2013 Conference on Advances in Liquid Scintillation Spectrometry, Barcelona, Spain, 18–22 March 2013, (proceedings will also be published in the Journal Applied Radiation and Isotopes, in preparation).
- Kossert, K., Nähle, O., Janßen, H., 2013. Activity determination of  $^{229}\text{Th}$  by means of LS counting. ICRM 2013, (accepted for publication).
- Lépy, M.-C., Cassette, Ph., Ferreux, L., 2010. Measurement of beta-plus emitters by gamma-ray spectrometry. Appl. Radiat. Isot. 68, 1423–1427.
- Mougeot, X., Bé, M.-M., Chisté, V., Dulieu, C., Gorozhankin, V., Loidl, M., 2011. Calculation of beta spectra for allowed and unique forbidden transitions. Proceedings of the 2010 International Conference on Liquid Scintillation Spectrometry, Paris, France, Radiocarbon, The University of Arizona, Tucson, Arizona, USA, ISBN: 978-0-9638314-7-7, pp. 249–257.
- Oropesa Verdecia, P., Kossert, K., 2009. Activity Standardization of  $^{131}\text{I}$  at CENTIS-DMR and PTB within the scope of a bilateral comparison. Appl. Radiat. Isot. 67, 1099–1103.
- Pochwalski, K., Broda, R., Radoszewski, T., 1988. Standardization of pure beta emitters by liquid scintillation counting. Appl. Radiat. Isot. 39, 165–172.
- Salvat, F., Fernandez-Varea, J.M., 2009. Overview of physical interaction models for photon and electron transport used in Monte Carlo codes. Metrologia 46, S112–S138.
- Salvat, F., Fernandez-Varea, J.M., Sempau, J., 2011. PENELOPE-2011, A Code System for Monte Carlo Simulation of Electron and Photon Transport. Tutorial for PENELOPE (version 2011).
- Schönfeld, E., Janßen, H., 1996. Evaluation of atomic shell data. Nucl. Instrum. Methods Phys. Res. A 369, 527–533.
- Tan, Z., Xia, Y., 2012. Stopping power and mean free path for low-energy electrons in ten scintillators over energy range of 20–20,000 eV. Appl. Radiat. Isot. 70, 296–300.